Investigation of the Carrier Concentration and Laser Peak Intensity on the Terahertz Pulse Generated by Photoconductive Antennas Based On LT-GaAs

Mohamad Ali Malakoutian[1], Morteza Fathipour[1]
1- Department of Electrical and Computer Engineering, University of Tehran, Tehran, Iran.
Email: m.a.malakoutian@ut.ac.ir

ABSTRACT:
The possibility of terahertz generation has been investigated from a photoconductive switch based on GaAs, gated by a femtosecond laser. The emission properties of photoconductive antenna (PCA) with low-temperature-grown (LT) GaAs have been studied. In such GaAs materials presence of the charged defects induces a redistribution of the electric field between the antenna electrodes. This effect has a huge influence on the amplitude of the radiated terahertz field. In this work we demonstrate that carrier concentration enhances radiation power. Results obtained as a function of the laser excitation power (with 100 fs rise time and 1KHz repetition rate) and carrier concentration are discussed and a comparison of the performance of these devices with a conventional antenna-type (dipole) emitter is given.

KEYWORDS: Photoconductive antennas (PCAs), LT-GaAs, THz radiation, Femtosecond laser.

1. INTRODUCTION

Terahertz (THz) radiation systems have received much interest in recent years. There have been new breakthroughs in generation, detection and fabrication of optical elements (such as waveguides, wave plates, filters, etc.) motivated by a wide range of applications spanning from analytical instrument in science to high-speed communication technology. During the last decade, the general interest in THz radiation rose significantly, mainly due to its ability to penetrate many organic materials, without introducing any damage usually associated with ionizing radiation such as X-rays. Since THz radiation is strongly absorbed by water molecules, it can be used to distinguish between materials with varying water content. All these properties laid the grounds for extensive applications in process and quality control [1] as well as biomedical imaging (T-ray imaging) [2]. Tests are currently under way to determine whether terahertz tomographic imaging can augment or replace mammography [3]. Scientists have proposed terahertz imaging as a method for screening passengers for explosives at airports [4]. The generation of THz radiation has been achieved by various techniques, such as ultrafast switching of photoconductive antennas [6, 7], rapid screening of the surface field via photoexcitation of dense electron hole plasma in semiconductors [8], rectification of optical pulses in crystals [9], carrier tunneling in coupled double-quantum well structures [10] and coherent excitation of polar optical photons [11]. Some of III-V group materials can be processed to obtain high resistivity and reasonably good carrier mobility, in addition to short carrier lifetime (<1 ps). These excellent characteristics are appropriate for use PCAs. Most commonly used material reported as the substrate material for PCAs is the low-temperature (LT) grown GaAs. This material exhibit good structural and electrical properties, and shows ultrafast optoelectronic response.

The mechanism of generation of THz radiation from biased photoconductors is generally understood based on the current surge model [12]. In this model, a THz electromagnetic field is radiated from a transient current generated on the surface of a photoconductor. Ultra short optical pulses generate carriers almost instantaneously and the carriers are accelerated by the local electric field. The resultant transient current, or current surge, produces an electric field on the surface of the photoconductor and this surface field can be regarded as the source of the THz radiation. The surface field, at the same time, partly cancels the bias field applied to the photoconductor. This is called the near-field screening effect. A theoretical treatment of the THz radiation generation process incorporating the near-field screening effect has explained these phenomena successfully. These studies, however, used relatively small gap spacing, which ranged from 5 µm to 20 µm. The spatial distribution of the bias field between the electrodes is dependent on the size and shape of both the photoconductor and the electrodes.

In this work, we investigated THz radiation from a micrometer-sized GaAs photoconductive antenna and observed the waveforms of the current through the contacts. We have analyzed the FWHM parameter of transient response to determine the band width of the photoconductive device. In section 2 the modeling of current, electric field, magnetic field and generation process is described, and in section 3 results of simulation is discussed.

2. PCA MODELING

Fig. 1 shows the structure of a dipole antenna used in our analysis where the parameters are a=50µm, b=50µm, c=50µm, d=20µm, and e=10µm. The simulation process starts by initializing the steady-state solutions of electric field E_0 and carrier densities n_0, p_0. After steady-state simulation we increased the anode voltage to 100V before illuminating the laser pulse. The 3D Poisson's equation in first is solved for the distribution profile of internal potential ψ within the device:

$$\frac{\partial^2\psi}{\partial x^2}+\frac{\partial^2\psi}{\partial x^2}+\frac{\partial^2\psi}{\partial x^2}=-\frac{q}{\varepsilon_s}[p-n+N_D-N_A] \qquad (1)$$

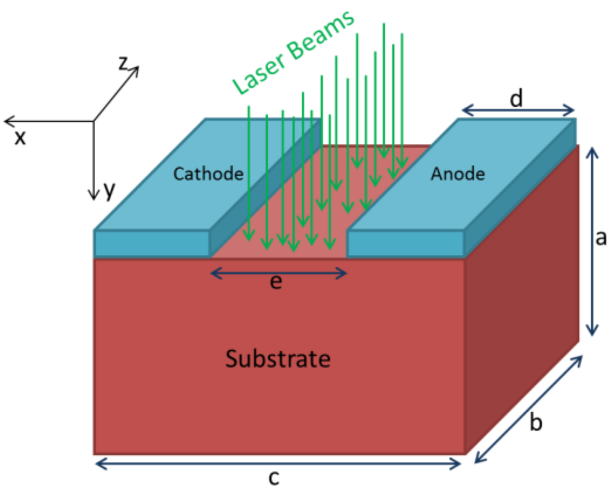

Fig. 1. Dipole antenna structure with dimensions.

Where p and n are the hole and electron concentrations, respectively, N_D-N_A is the concentration of impurities, q is the electron charge, and ε_s are the permittivity of the device substrate. The steady-state E_0, n_0, and p_0 are the initial conditions and are determined using the potential ψ obtained from (1). By changing the n and p in this equation, ψ is changed.

We use time-domain calculations for determination of the electric field pattern of the antenna by using equations from (2) through (5). These equations are Maxwell, Drift-Diffusion, and Generation-Recombination's equations [13], [14]. Electric and Magnetic fields are calculated as:

$$\nabla\times\vec{E}(t)=-\mu\frac{\partial\vec{H}(t)}{\partial t} \qquad (2.1)$$

$$\nabla\times\vec{H}(t)=\varepsilon\frac{\partial\vec{E}(t)}{\partial t}+\vec{J_n}(t)+\vec{J_p}(t) \qquad (2.2)$$

Where *E(t)* is the variable electric field, *H(t)* is the magnetic field, $J_n(t)$ and $J_p(t)$ are electron and hole current densities, µ and ε are the permeability and permittivity of the medium respectively.

We use equation (3) and (4) to calculate the current densities:

$$q\frac{\partial n(t)}{\partial t}=\nabla.\vec{J_n}(t)+qG-qR \qquad (3.1)$$

$$q\frac{\partial p(t)}{\partial t}=-\nabla.\vec{J_p}(t)+qG-qR \qquad (3.2)$$

$$\vec{J_n}(t)=q\mu_n n(t)[E_0+E(t)]-qD_n\nabla n(t) \qquad (4.1)$$

$$\vec{J_p}(t)=q\mu_p p(t)[E_0+E(t)]-qD_p\nabla p(t) \qquad (4.2)$$

Where μ_n and μ_p is the electron and hole mobilities, D_n and D_p is the Einstein diffusion coefficients for electron and hole, and G and R represent, the carrier generation rate and the recombination rate, respectively.

In this paper, these four equations are solved self consistently using iterative methods on the three dimensional simulation region to calculate electron and hole currents resulting from the incident laser pulse.

Finally for calculating the rate of carrier generation and recombination, we use the equation (5):

$$G(x,y,z,t)= G_0\exp\left(-\alpha(z-z_0)\right).\exp\left(-\frac{(x-x_0)}{\sigma_x^2}-\frac{(z-z_0)}{\sigma_z^2}\right) .\exp\left(-\frac{\left(t-(z-z_0)\frac{\sqrt{\varepsilon_s}}{c}-t_0\right)^2}{\sigma_t^2}\right) \qquad (5)$$

Where α is the absorption coefficient, c is the velocity of light in vacuum. The parameter G_0 depends on α and photon energy. The first exponential term in (5) is for light penetration into the substrate, second exponential term is the radial excitation area, and third term is the temporal shape of the optical pulse. At high electric fields carrier velocities will begin to saturate as a result of low effective carrier mobility values. This effect has been included by use of the Caughey and Thomas field-dependent mobilities model [13]. The recombination rate, *R*, was modeled using the Shockley- Read-Hall (SRH) process.

3. RESULTS AND DISCUSSIONS

The output power of the emitted far-field THz pulse is affected by the applied bias voltage, carrier concentration of the substrate, pulsed laser intensity, antenna type, and carrier mobility of the photoconductor material. In this work we investigated the effect of carrier concentration of the substrate and pulsed laser intensity, on peak current density and FWHM of PCA.

3.1. Carrier Concentration

By increasing the carrier concentration of the body the peak value of current density is increased, as shown in Fig. 2. This occurs as a result of increase in the *p(t)* and *n(t)* terms in current density equation (4). The FWHM parameter of each device is decreased by increase in carrier concentration. Shorter rise time and higher peak value result in larger FWHM, but longer settling time for lower carrier concentrations is a crucial parameter which determines the FWHM. Table 1 shows the peak current and FWHM values for each device. The peak intensity of the laser source and the bias voltage for all simulations is 50MW/cm^2 and 100V respectively.

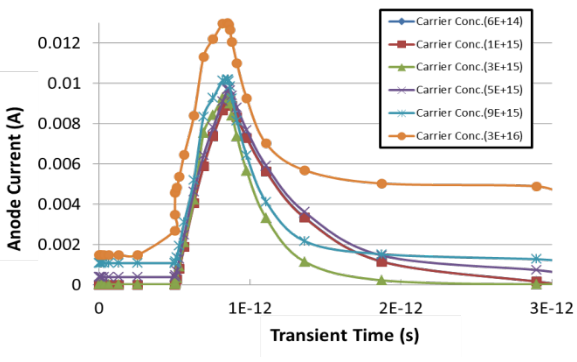

Fig. 2. Anode current versus transient time for b=1µm.

Table 1. Peak current and FWHM parameters for b=50µm.

Carrier Conc. (cm^{-3})	Peak Current (mA)	FWHM (fs)
$6x10^{14}$	451	655
$1x10^{15}$	459	650
$3x10^{15}$	466	641
$5x10^{15}$	486	589
$9x10^{15}$	505	533
$3x10^{16}$	650	490

Shorter FWHM can force the device to work on wider bandwidth frequency range.

3.2. Laser Peak Intensity

In this section we investigate the effect of peak intensity of the laser source on the amount of peak current density and FWHM parameter (table 2). Fig. 3 shows increasing of the peak current to 466.5 mA, and of the FWHM parameter to 577 fs, by increasing the peak intensity of the laser.

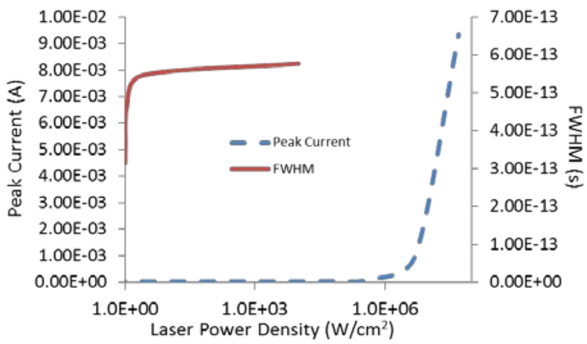

Fig. 3. Peak current and FWHM versus laser power density for b=1µm.

Table 2. Peak current and FWHM parameters for b=50µm.

Laser Intensity (W/cm^2)	Peak Current (mA)	FWHM (fs)
0.5	1.65	315
5	1.65	321
50	1.65	322
500	1.655	325
5k	1.67	330
50k	1.93	358
500k	6	465
5M	50.5	546
50M	466.5	577

4. CONCLUTION

We have investigated the properties of THz emission from biased, micrometer-sized photoconductors excited by trains of amplified fs optical laser pulses. These results can be used in the design of optimal emitters to generate high-energy THz pulse trains for applications in communications, nonlinear optics, and coherent control. We have simulated the characteristics of a series of PC antenna-type emitters fabricated on different carrier concentration substrates. In all cases, increasing the carrier concentration allows us to obtain a higher THz radiation intensity in the saturation regime, and wider bandwidth for our emitters. In addition by increasing the power of laser source, as we expected, peak current and FWHM parameter are increased, this means that the bandwidth of the antenna was decreased. A better knowledge of the nature of the defects and their spatial distributions could help to design optimized materials having short carrier lifetime, high carrier mobility, and the presence of a region of high electric field.

REFERENCES

[1] T. Lo er, K.J. Siebertt, N. Hasegawa, T. Hahn, G. Loata, R. Wipf, M. Kress, M. Thomson, and H.G Roskos, "Terahertz surface and interface characterization", 2005 IEEE MTT-S International Microwave Symposium Digest, pages 4, 2005.

[2] B. Ferguson, S. Wang, D. Gray, D. Abbott, and X-C Zhang, "Towards functional 3d t-ray imaging", Phys. Med. Biol, 47:3735_3742, 2002.

[3] Anthony J. Fitzgerald, Vincent P. Wallace, Mercedes Jimenez-Linan, Lynda Bobrow, Richard J. Pye, Anand D. Purushotham, and Donald D. Arnone, "Terahertz Pulsed Imaging of Human Breast Tumors", Radiology, 239(2):533_ 540, 2006.

[4] William R. Tribe, David A. Newnham, Philip F. Taday, and Michael C. Kemp, "Hidden object detection: security applications of terahertz technology", In R. Jennifer Hwu, editor, Proceedings of SPIE, volume 5354 of Terahertz and Gigahertz Electronics and Photonics III, pages 168_176, 2004.

[5] J. F. Fuller, E. F. Fuchs, and K. J. Roesler, "Influence of harmonics on power distribution system protection," IEEE Trans. Power Delivery, vol. 3, pp. 549-557, Apr. 1988.

[6] Auston, D.H., Cheung, K.P., and Smith, P.R.: "Picosecond photoconducting hertzian dipoles", Appl. Phys. Lett., 1984, 45, (3), pp. 284–286

[7] Grischkowsky, D., Keiding, S., Vanexter, M., and Fattinger, "Far-infrared time-domain spectroscopy with terahertz beams of dielectrics and semiconductors", J. Opt. Soc. Am. B, 1990, 7, (10), pp. 2006–2015

[8] Zhang, X.C., and Auston, "Optoelectronic measurement of semiconductor surfaces and interfaces with femtosecond optics", J. Appl. Phys., 1992, 71, (1), pp. 326–338

[9] Hu, B.B., Zhang, X.C., Auston, D.H., and Smith, "Free-space radiation from electrooptic crystals", Appl. Phys. Lett., 1990, 56, (6), pp. 506–508

[10] Roskos, H.G., Nuss, M.C., Shah, J., Leo, K., Miller, D.A.B., Fox, A.M., Schmit-Trink, S., and Kohler, "Coherent submillimeter-wave emission from charge oscillations in a double-well potential", Phys. Rev. Lett., 1994, 68, (14), pp. 2216–2219

[11] Tani, M., Fukasawa, R., Abe, H., Matsuura, S., Sakai, K., and Nakashima, "Terahertz radiation from coherent phonons excited in semiconductors", J. Appl. Phys., 1998, 83, (5), pp. 2473–2477.

[12] J. T. Darrow, X.-C. Zhang, D. H. Auston and J. D. Morse: IEEE J. Quantum Electron. 28 (1992) 1607.R.

[13] D. M. Caughey and R. E. Thomas, "Carrier mobilities in silicon empirically related to doping and field," Proc. IEEE, vol. 55, pp. 2192-2193, 1967.

[14] R. Luebbers, K. Kunz, M. Schneider, and F. Hunsberger, "A finitedifference time-domain near zone to far zone transformation", IEEE Trans. Antennas. Propagat., vol 39, no 4, pp 429-433, April 1991.